Propagation of a weakly nonlinear laser pulse in a curved plasma channel

A. J. W. Reitsma and D. A. Jaroszynski
Department of Physics, University of Strathclyde, Glasgow G4 0NG, United Kingdom

(Received 16 March 2007; accepted 22 March 2007; published online 14 May 2007)

In this paper, the propagation of a high intensity laser pulse in a curved plasma channel is studied. The matching conditions, which are different from straight plasma channels, are examined. The analysis includes a study of centroid and spot size oscillations, relativistic self-focusing, and the effect of wakefields on the propagation of the laser pulse. The possible application of curved plasma channels in laser wakefield acceleration is discussed. © *2007 American Institute of Physics*. [DOI: 10.1063/1.2731816]

I. INTRODUCTION

Plasma channels play an important role in laser-plasma interaction, as they offer a practical solution to the problem of extending the interaction length beyond the limit set by geometric diffraction.[1,2] A plasma channel can be employed as an efficient medium for x-ray lasing,[3] harmonic generation,[4] or Raman amplification.[5] Furthermore, a recent experiment demonstrated GeV electron acceleration in a channel-guided laser wakefield accelerator for the first time.[6] The principle behind plasma channel guiding is that a plasma column that has a radial density profile with an on-axis minimum can, through the dependence of refractive index on plasma density, act as a lens for laser light.[7] Guiding over long distances is possible due to a balance between the inward bending of light rays through the refractive index gradient and the outward expansion through geometric diffraction.

The laser can propagate without significant spot size or centroid oscillations if it couples into a single eigenmode of the channel, in which case it is said to be *matched*. However, for different spot sizes, off-axis injection or injection under an angle with the channel axis, sizeable spot size or centroid oscillations do occur, and the pulse is called *mismatched*. Mismatched injection may lead to loss of pulse intensity. Plasma channel guiding is not the only way to achieve a long laser-plasma interaction length: alternative methods include capillary guiding (relying on total internal reflection on the capillary boundary),[8] relativistic self-focusing,[9] and laser pulse shaping.[10]

As with other types of waveguides, such as optical fibers, it is possible with a plasma channel to guide the light along a curved path by bending the waveguide. This has been experimentally demonstrated by Ehrlich *et al.* for laser pulses with relatively low peak intensities (up to 10^{16} W cm^{-2}).[11] The authors provide an analytical estimate for the minimum radius of curvature for confinement of the laser pulse to the curved channel. In this paper we discuss the weakly nonlinear regime (laser peak intensities around 10^{17} W cm^{-2}), for which relativistic and ponderomotive effects start to play a role. We expect that it is not possible to bend laser pulses in the strongly nonlinear regime (peak intensity 10^{18} W cm^{-2} and above) in curved plasma channels, as it becomes increasingly difficult to radially confine the laser pulse. Furthermore, strong coupling with the wakefield will lead to large losses and pulse deformation. The motivation for this work is to investigate the use of curved plasma channels for electron acceleration, as, for example, the ability to bend the laser light and/or the electron bunch may be interesting for the design of a multistage laser wakefield accelerator. In this paper we only address the propagation of the laser pulse, leaving the electron acceleration dynamics for possible future investigation.

The outline of this paper is as follows. In Sec. II, the envelope equation for a laser pulse propagating in a curved plasma channel is derived. Subsequently, this equation is studied in paraxial approximation in Sec. III and finite pulse length effects are included in Sec. IV. Section V is devoted to summary and discussion.

II. ENVELOPE EQUATION

In this section, we derive an envelope equation to describe the evolution of a laser pulse that propagates in a circular plasma channel. We simplify the geometry of the problem by setting $\partial/\partial y=0$ in all equations. Generalization to three-dimensional geometry, for example, a plasma channel with a toroidal shape, is straightforward (see the Appendix). A radial coordinate r is defined as $r=(x^2+z^2)^{1/2}-R$ with R the radius of the plasma channel and the plasma density is assumed to be parabolic close to $r=0$: $n_p(r)=n_0(1+r^2/r_c^2)$, where $r_c \ll R$ determines the curvature of the parabolic density profile. A laser pulse with linear polarization in the y direction is assumed, and the evolution of the vector potential is described with the wave equation $(c^2\nabla^2-\partial^2/\partial t^2)A_y=\omega_p^2 A_y$, where $\omega_p^2=4\pi n_p e^2/m_e$ defines the r-dependent plasma frequency ω_p. We introduce the obvious change of coordinates $(x,z)\rightarrow[r,\phi=\arctan(x/z)]$, and assume that A_y is the product of a slowly varying envelope and a rapidly varying carrier wave $eA_y/mc^2=(1/2)[a(r,\phi,t)\exp(ik_0R\phi-i\omega_0 t)+\text{c.c.}]$, where a is given in dimensionless form. Furthermore, we introduce a co-moving coordinate $s=R\phi-ct$, and find that

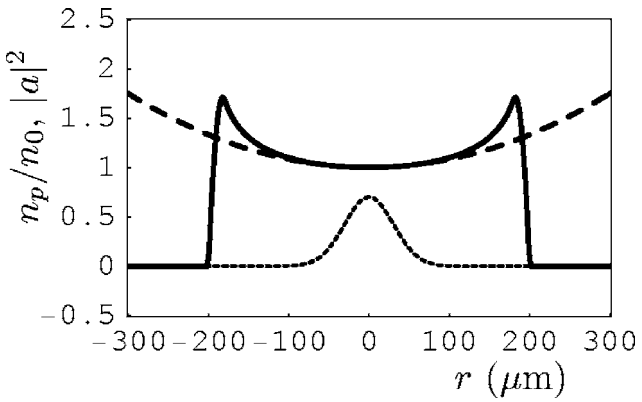

FIG. 1. Radial density profile used in this paper (solid line), parabolic approximation (dashed line) and intensity profile of matched Gaussian pulse (dotted line).

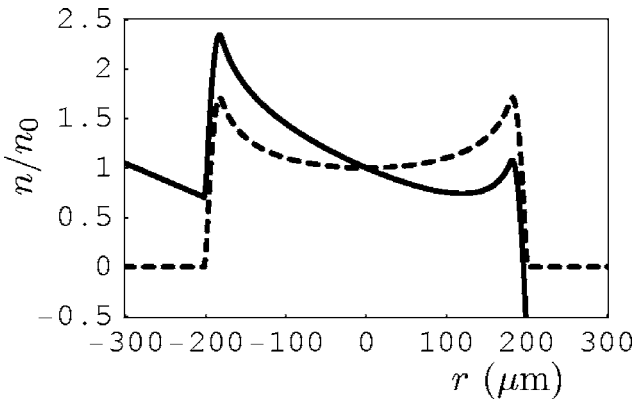

FIG. 3. Radial density profile of Fig. 1 (dashed line) and effective density profile of curved channel with $R=1$ m (solid line).

$$\left\{c^2\left[\frac{\partial^2}{\partial r^2}+\frac{1}{R+r}\frac{\partial}{\partial r}+\frac{R^2}{(R+r)^2}\left(\frac{\partial^2}{\partial s^2}+2ik_0\frac{\partial}{\partial s}-k_0^2\right)\right]\right.$$
$$\left.-\left[\frac{\partial^2}{\partial t^2}-2c\frac{\partial^2}{\partial s\partial t}+c^2\frac{\partial^2}{\partial s^2}-2i\omega_0\frac{\partial}{\partial t}+2ci\omega_0\frac{\partial}{\partial s}-\omega_0^2\right]\right\}a$$
$$=\omega_p^2 a. \quad (1)$$

In the limit $R\to\infty$, the usual envelope equation is recovered:[12]

$$\left[2i\omega_0\frac{\partial}{\partial t}+2c\frac{\partial^2}{\partial s\partial t}+c^2\frac{\partial^2}{\partial r^2}\right]a=\omega_p^2 a, \quad (2)$$

where $\omega_0=ck_0$ (approximation of very underdense plasma) has been used, and a second-order t derivative has been omitted (slowly varying envelope approximation).

III. PARAXIAL APPROXIMATION

As a first step, effects related to finite laser pulse length have been omitted; i.e., $\partial/\partial s=0$ is assumed (paraxial approximation). Keeping terms to lowest order in r/R gives

$$\left(2i\omega_0\frac{\partial}{\partial t}+c^2\frac{\partial^2}{\partial r^2}\right)a=\left(\omega_p^2-2\omega_0^2\frac{r}{R}\right)a. \quad (3)$$

From the similarity between Eq. (3) and the one-particle Schrödinger equation, one can see that the quantity between brackets on the right-hand side of the equation plays the role of a potential. Therefore, it makes sense to introduce an effective density $n=n_p-2n_{cr}r/R$, which is proportional to this potential, where n_{cr} is the critical density. The minimum of the effective density, which defines the equilibrium position of the laser pulse, is located at $r=(\omega_0/\omega_{p0})^2r_c^2/R$, where $\omega_{p0}=\omega_p(r=0)$. This implies that a laser pulse injected around $r=0$, which is the usual condition for matching in a straight channel, will be mismatched and undergo a radial oscillation around the equilibrium position. If the amplitude of this oscillation is large, the approximation of a parabolic channel may break down. In a realistic plasma channel, this would lead to attenuation of the laser pulse due to leakage from the channel. The shift in equilibrium position should be small compared with the channel radius, which requires $r_c/R\ll(\omega_{p0}/\omega_0)^2$. This is a much stronger requirement than the condition $r_c/R\ll1$ stated above. We illustrate this point by introducing a realistic density profile in Fig. 1, which is modeled after the profile of a slow capillary discharge plasma channel[13,14] with a 200 μm radius. Also given in Fig. 1 are the parabolic approximation (with parameters $n_0=10^{18}$ cm^{-3}, $r_c=346$ μm) and the radial intensity distribution of a Gaussian pulse that is matched to the parabolic density profile. For comparison, we show the result of a simulation of Eq. (3) in a straight channel ($R\to\infty$) with initial condition

$$a(r)=a_0\exp[-(r-r_0)^2/(2r_1^2)] \quad (4)$$

is shown in Fig. 2. The parameters for this simulation are $r_0=0$ (on-axis injection), $r_1=(cr_c/\omega_{p0})^{1/2}=43$ μm (condition for a matched pulse in a parabolic channel): $a_0^2=0.5$. In all simulations presented in this paper, the realistic density profile of Fig. 1 is used, *not* the parabolic approximation. Figure 2 merely illustrates the point that this makes little difference for a straight channel, as perfect guiding is observed over a long propagation distance, albeit with a slight spot size oscillation.

Now let us investigate the propagation in a curved channel with $R=1$ m, corresponding to the effective density profile of Fig. 3, which shows a relatively large shift in equilibrium position, consistent with $r_c/R=0.6(\omega_{p0}/\omega_0)^2$. Therefore, if we use the same initial conditions for the laser pulse as before ($r_0=0$ μm, $r_1=43$ μm, $a_0^2=0.5$), it is not surprising to observe strong centroid and spot size oscillations,

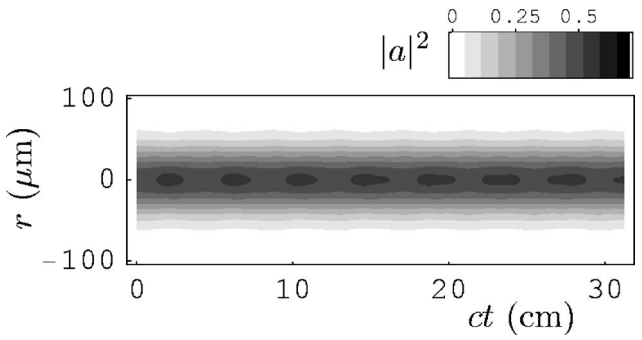

FIG. 2. Simulation result of matched pulse in straight channel with $r_0=0$, $r_1=43$ μm, and $a_0^2=0.5$.

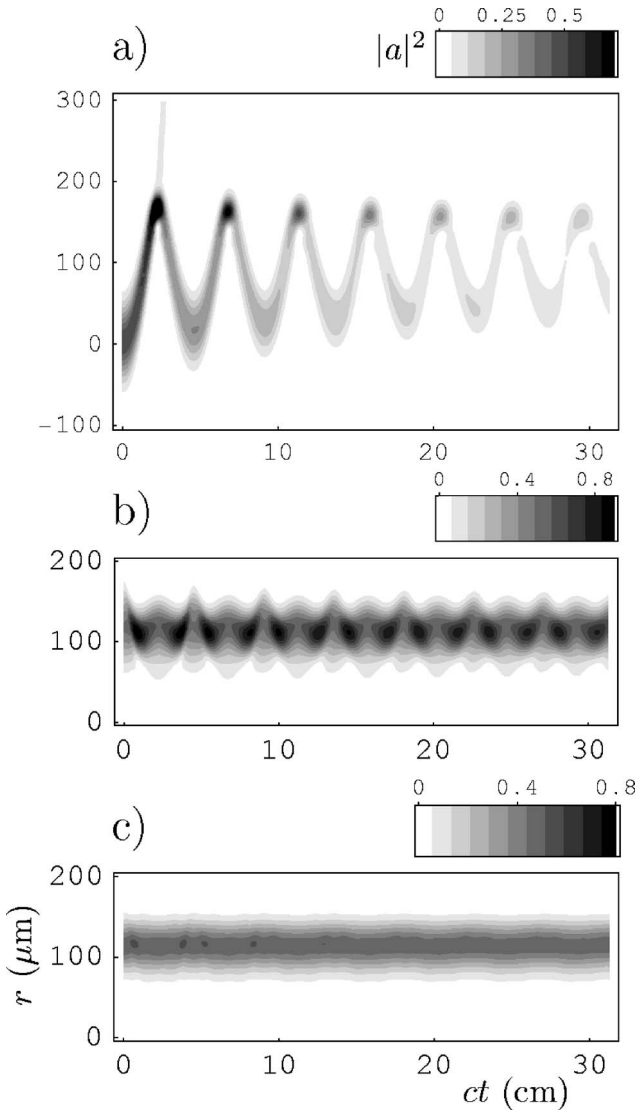

FIG. 4. Simulation results of pulse propagation in curved channel with $R=1$ m. Plot (a) corresponds to $r_0=0$, $r_1=43$ μm; plot (b) to $r_0=120$ μm, $r_1=43$ μm; and plot (c) to $r_0=115$ μm, $r_1=30$ μm. For all plots, $a_0^2=0.5$.

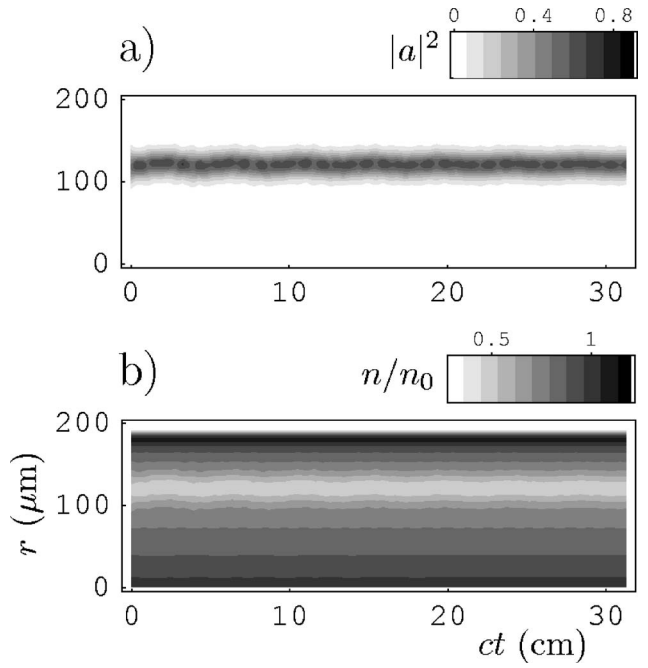

FIG. 5. Simulation result of pulse propagation in curved channel, including relativistic self-focusing, showing the evolution of (a) the vector potential envelope $|a|^2$ and (b) the effective density n. Parameters: $r_0=120$ μm, $r_1=20$ μm, and $a_0^2=0.5$.

as well as loss of laser pulse intensity due to leakage of radiation, as shown in Fig. 4(a). In order to avoid centroid oscillations altogether, we propose to inject the laser pulse off-axis, around the equilibrium position. Fig. 4(b) shows the simulation result for $r_0=120$ μm (the local minimum of the effective density), $r_1=43$ μm, and $a_0^2=0.5$. We still observe centroid and spot size oscillations, but they are not as severe as those found in Fig. 4(a). In addition, there is no appreciable attenuation. We do, however, observe a periodic deformation of the pulse shape from Gaussian into different asymmetric shapes. This is most likely caused by the asymmetric form of the effective density (Fig. 3), for which the parabolic approximation is valid in a much smaller region around the equilibrium position than in the case of a straight channel (Fig. 1). In addition, the curvature at the equilibrium position is larger for the curved channel than for the straight channel. Thus, it should be possible to reduce centroid and spot size oscillations even further by using a smaller spot size and perhaps adjusting the injection position. This is confirmed by the simulation result shown in Fig. 4(c), which corresponds to $r_0=115$ μm and $r_1=30$ μm. Note also that there is much less pulse shape deformation than in Fig. 4(b).

For a laser pulse in the relativistic regime (i.e., a_0 of order 1) one has to consider the effect of *self-focusing*. For simplicity, we consider only *relativistic* self-focusing, i.e., the change of refractive index due to the relativistic mass correction that stems from the quiver motion, and leave out *ponderomotive* self-focusing; i.e. radial electron blowout due to the light pressure. For a thorough discussion of both types of self-focusing, see Refs. 15 and 16. Relativistic self-focusing is modeled by changing the $\omega_p^2 a$ term in Eq. (3) to $\omega_p^2 a/(1+|a|^2)^{1/2}$. As a consequence, the effective density becomes $n=n_p/(1+|a|^2)^{1/2}-2n_{cr}r/R$. As we expect, the matched spot size for the self-focusing case to be smaller than without self-focusing,[15,16] we select the initial conditions $r_0=120$ μm, $r_1=20$ μm for two different pulse intensities, corresponding to $a_0^2=0.5$ and $a_0^2=1.2$, and present the simulation results in Figs. 5 and 6, respectively. These figures show the evolution of $|a|^2$ and the density. Due to the feedback from the laser pulse on the effective density, the centroid and spot size oscillations are seen to be damped, and the system evolves towards an equilibrium. At high intensity (the case $a_0^2=1.2$) we observe that the equilibrium position is further from the axis and the equilibrium spot size is smaller than at low intensity ($a_0^2=0.5$). These results can be understood as follows. If the peak of the laser pulse is at the equilibrium position, i.e., at the minimum of the effective density, then that position is found to be

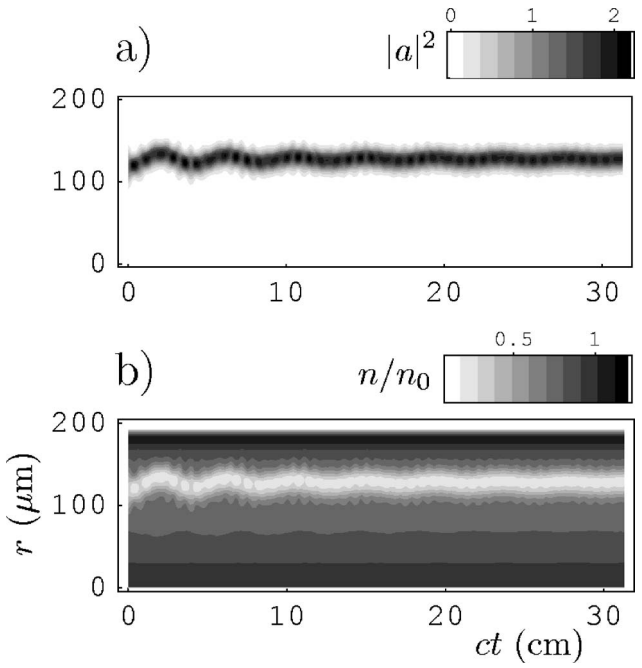

FIG. 6. As Fig. 5, with $a_0^2=1.2$.

$$r_0=(1+a_0^2)^{1/2}\left(\frac{\omega_0}{\omega_{p0}}\right)^2\frac{r_c^2}{R}, \tag{5}$$

where we have used a parabolic shape for the channel and Eq. (4) for the laser pulse. Thus, the equilibrium position r_0 is seen to be further from the axis than in the case without self-focusing, and more and more so with increasing pulse intensity. This confirms that very intense pulses cannot be confined in curved plasma channels due to self-focusing effects, as stated in Sec. I. Close to $r=r_0$ we may write the effective density as $n/n_0=C+(r-r_0)^2/\bar{r}_c^2$, where $C=(1-r_0^2/r_c^2)/(1+a_0^2)^{1/2}$ is a constant and $\bar{r}_c$ determines the curvature:

$$\bar{r}_c^2=\frac{(1+a_0^2)^{3/2}r_c^2}{1+a_0^2+a_0^2(r_0^2+r_c^2)/(2r_1^2)}. \tag{6}$$

The matching condition for the laser spot size is $r_1=(c\bar{r}_c/\omega_{p0})^{1/2}$, which can be used to determine $\bar{r}_c$ from Eqs. (5) and (6). It is found that $\bar{r}_c/r_c$ is smaller than 1 and decreases with increasing a_0. This implies that the spot size is smaller than without self-focusing, and decreases with increasing intensity.

IV. FINITE PULSE LENGTH

We retain the longitudinal dependence in Eq. (1) and model the energy loss to the plasma by taking into account the effect of the wakefield. Again, we assume to be in a weakly nonlinear regime, so that a linear hydrodynamic description of the wakefield is adequate, in which case the equation for the plasma velocity $\mathbf{v}$ is[17]

$$\frac{\partial^2\mathbf{v}}{\partial t^2}+\omega_p^2\mathbf{v}+c^2\boldsymbol{\nabla}\times[\boldsymbol{\nabla}\times\mathbf{v}]=-c^2\frac{\partial}{\partial t}\boldsymbol{\nabla}\frac{|a|^2}{4}.$$

Replacing the (ϕ,t) dependence with dependence on s only (quasistatic approximation), it is found that

$$c^2\left[\frac{\partial^2 v_r}{\partial s^2}+\frac{R}{R+r}\frac{\partial^2 v_\phi}{\partial r\partial s}+\frac{R^2}{(R+r)^2}\frac{\partial}{\partial s}\left(\frac{v_\phi}{R}-\frac{\partial v_r}{\partial s}\right)\right]+\omega_p^2 v_r=c^3\frac{\partial^2}{\partial r\partial s}\frac{|a|^2}{4},$$

$$c^2\left[\frac{\partial^2 v_\phi}{\partial s^2}-\frac{\partial^2 v_\phi}{\partial r^2}+\frac{R}{R+r}\left(\frac{1}{R+r}-\frac{\partial}{\partial r}\right)\left(\frac{v_\phi}{R}-\frac{\partial v_r}{\partial s}\right)\right]+\omega_p^2 v_\phi=c^3\frac{R}{R+r}\frac{\partial^2}{\partial s^2}\frac{|a|^2}{4}.$$

In zeroth-order approximation, one recovers the usual wakefield equations[17]

$$v_r=-\frac{c^3}{\omega_p^2}\frac{\partial^2}{\partial r\partial s}\left(\frac{v_\phi}{c}-\frac{|a|^2}{4}\right)\equiv-\frac{c^3}{\omega_p^2}\frac{\partial^2}{\partial r\partial s}\psi,$$

$$\left[\frac{\partial^2}{\partial s^2}-\frac{\partial^2}{\partial r^2}-\frac{\partial^2}{\partial r\partial s}\left(\frac{c^2}{\omega_p^2}\frac{\partial^2}{\partial r\partial s}\right)+\frac{\omega_p^2}{c^2}\right]\psi=\left(\frac{\omega_p^2}{c^2}-\frac{\partial^2}{\partial r^2}\right)\frac{|a|^2}{4}. \tag{7}$$

Denoting the first-order contributions as $\tilde{v}_r$, etc. yields

$$\frac{\omega_p^2}{c^2}\tilde{v}_r-\frac{\partial^2\tilde{v}_\phi}{\partial r\partial s}=\frac{r}{R+r}\frac{\partial^2 v_\phi}{\partial r\partial s}-\frac{R}{(R+r)^2}\frac{\partial v_\phi}{\partial s}+\frac{R^2-(R+r)^2}{(R+r)^2}\frac{\partial^2 v_r}{\partial s^2},$$

$$\frac{\partial^2\tilde{v}_\phi}{\partial s^2}-\frac{\partial^2\tilde{v}_\phi}{\partial r^2}+\frac{\partial^2\tilde{v}_r}{\partial r\partial s}+\frac{\omega_p^2}{c^2}\tilde{v}_\phi=\frac{1}{R+r}\frac{\partial v_\phi}{\partial r}+\frac{R}{(R+r)^2}\frac{\partial v_r}{\partial s}+\frac{r}{R+r}\left(\frac{\partial^2 v_r}{\partial r\partial s}-\frac{c}{4}\frac{\partial^2|a|^2}{\partial s^2}\right).$$

Note that these contributions are interesting from a theoretical point of view: for $|a|^2$ symmetric around $r=0$, $\tilde{v}_r$ is symmetric, and $\tilde{v}_\phi$ anti-symmetric; i.e., opposite to the zeroth-order contributions. Nonetheless, because they are so much smaller than the zeroth-order contributions, we have left $\tilde{v}_r$ and $\tilde{v}_\phi$ out of our simulations. The envelope equation becomes, to lowest order in r/R,

$$\left(2i\omega_0\frac{\partial}{\partial t}+2c\frac{\partial^2}{\partial s\partial t}+c^2\frac{\partial^2}{\partial r^2}\right)a=\left[\Omega_p^2-2\frac{r}{R}\left(\omega_0^2-2ic\omega_0\frac{\partial}{\partial s}-c^2\frac{\partial^2}{\partial s^2}\right)\right]a. \tag{8}$$

Here, $\Omega_p(r,s,t)$ is a localized plasma frequency that takes into account the coupling between the laser pulse and the plasma wave. In terms of the wakefield potential, it is expressed as $\Omega_p^2=\omega_p^2(1-\psi)+c^2\partial^2\psi/\partial r^2$. We have numerically simulated laser pulse propagation by solving the coupled equations (7) and (8). A double Gaussian laser profile

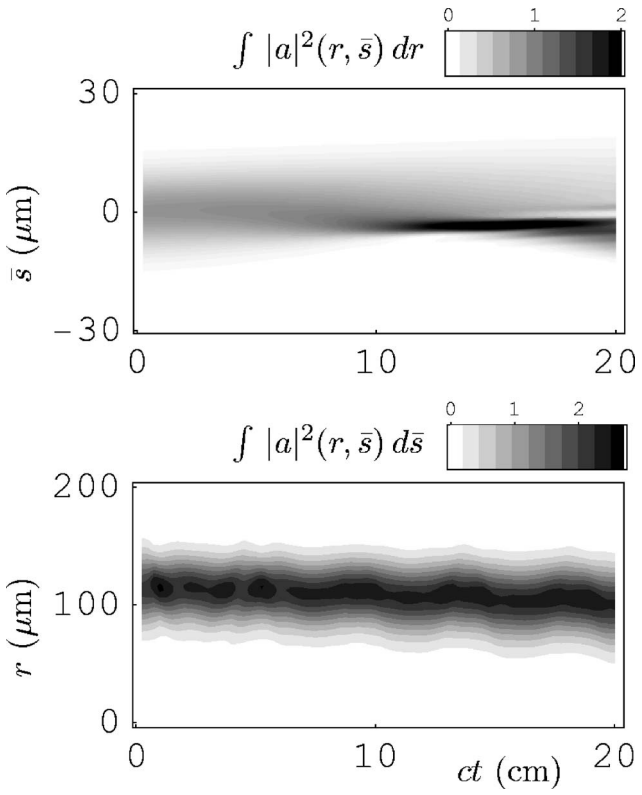

FIG. 7. Simulation result of two-dimensional code, showing longitudinal envelope dynamics ($|a|^2$ integrated over r) and transverse envelope dynamics ($|a|^2$ integrated over $\bar{s}$). Laser pulse parameters are $a_0^2=0.05$, $s_1=9$ μm, $r_0=115$ μm, and $r_1=30$ μm, corresponding to matched propagation in paraxial simulations (see Fig. 4). For definition of co-moving coordinate $\bar{s}$, see text.

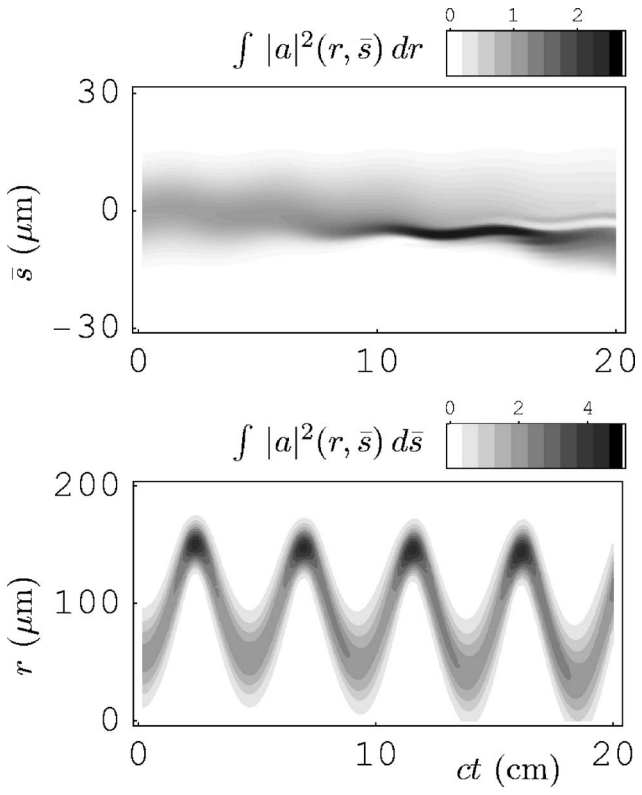

FIG. 8. As Fig. 7 with $r_0=55$ μm and $r_1=35$ μm, corresponding to mismatched pulse.

$$a(r,s) = a_0 \exp[-(r-r_0)^2/(2r_1^2) - s^2/(2s_1^2)] \tag{9}$$

is taken as initial condition, with $s_1=9$ μm, $a_0^2=0.05$, $r_0=115$ μm, and $r_1=30$ μm (matched pulse conditions taken from Sec. III), and $r_0=55$ μm, and $r_1=35$ μm (mismatched pulse). The simulation results are presented in Figs. 7 and 8 in the form of contour plots of $|a|^2$ integrated over r and s, which reveal the longitudinal and transverse envelope dynamics. In these figures, it is convenient to use a longitudinal coordinate $\bar{s}=R\phi-\bar{v}t$ to cancel the slippage that occurs in the $s=R\phi-ct$ frame. This slippage is partly due to the laser pulse group velocity being less than c, and partly a geometric effect, as points of constant s move with velocity $(1+r/R)c$ in the ϕ direction. For our simulations, it turns out that $\bar{v}/c=(1-1/\bar{\gamma}^2)^{-1/2}$ with $\bar{\gamma}\approx 33$ is a good choice to track the laser pulse (for comparison, $\omega_0/\omega_{p0}\approx 41$).

As expected, the $\int|a|^2 d\bar{s}$ plots of the transverse envelope dynamics show large centroid oscillations in the case of a mismatched pulse (Fig. 8), and relatively small centroid and spot size oscillations for a matched pulse (Fig. 7). An interesting feature in both plots is a *drift* of the centroid towards the channel axis, which was not observed in the simulation results presented in the previous section. To explain the origin of this feature, we plot $|a|^2$ and the effective density for the matched laser pulse at $t=0$ in Fig. 9. The plot of the effective density $n=n_p(1-\psi)+(mc^2/4\pi e^2)\partial^2\psi/\partial r^2-2n_{cr}r/R$ shows that the wakefield wave fronts are curved, as expected for a laser pulse in a plasma channel.[17] As a result of this curvature the equilibrium position, i.e., the local minimum of the effective density in the r direction, varies with s. This makes it impossible to perfectly match a laser pulse of the form of Eq. (9) everywhere along its length. In our simulations for example, the pulse is injected around $r_0=115$ μm, so that the head of the laser pulse is matched to the unperturbed effective density and this part of the pulse can propagate without centroid oscillations, in accordance with the simulation results presented in Sec. III. However, because of the curved wakefield the tail of the pulse is mismatched and undergoes centroid oscillations. The net effect of multiple centroid oscillations is the drift towards the channel axis that we observe in Figs. 7 and 8. Similar effects can occur in a straight plasma channel if the laser pulse is injected off-axis or becomes susceptible to the hosing instability.[18] It is interesting to note that perfect matching, which would avoid both centroid and spot size oscillations, in general is impossible for relativistic pulses, even in a straight plasma channel.

The $\int|a|^2 dr$ plots of the longitudinal envelope dynamics show the formation of a narrow peak towards the end of the pulse at about $ct=13$ cm and a subsequent broadening of this feature. This behavior is typical for the evolution of the laser pulse in a resonant laser wakefield accelerator, which has an initial pulse length of about half of the plasma wavelength to maximize the wakefield amplitude. In our case the initial pulse length is only slightly longer, and the pulse evolution is very similar.[19] The peak formation is a characteristic of an explosive instability caused by the mutual interaction between the laser pulse and its own wakefield.[20] The most

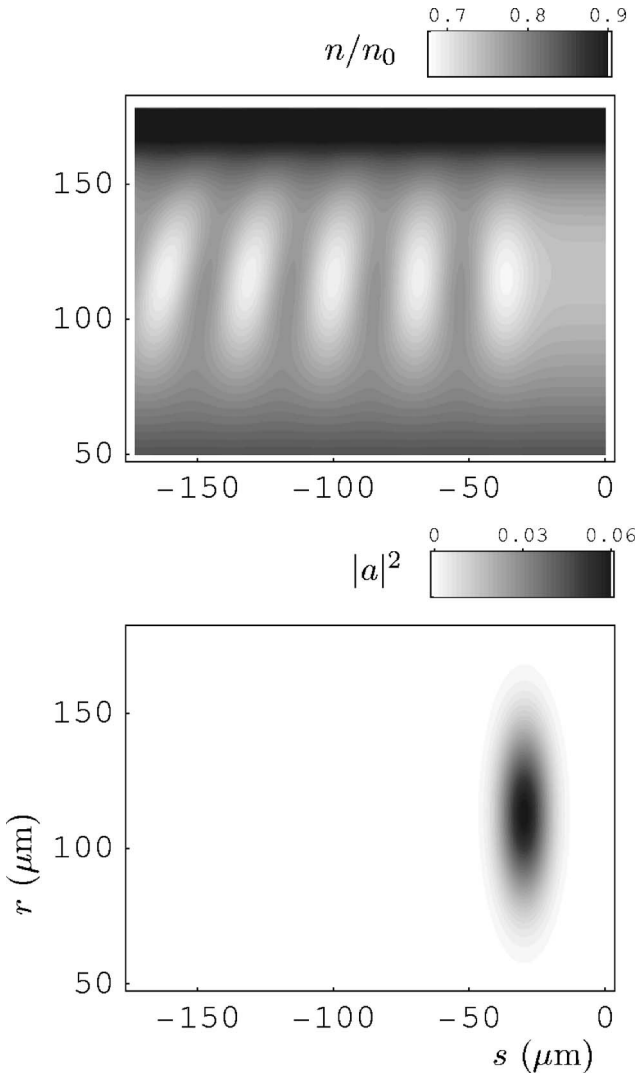

FIG. 9. Profiles of $|a|^2$ and effective density n as functions of r and s at $t=0$ for the simulation of Fig. 7. This plot illustrates the curvature of wakefield wave fronts resulting from the radial density profile.

striking difference between the longitudinal dynamics plots of Figs. 7 and 8 is the pulse oscillation observed in Fig. 8. This is most likely caused by the geometric effect described above: points of constant s (or $\bar{s}$) have a velocity in the ϕ direction that depends on r, so if the pulse experiences appreciable centroid oscillations, as observed in the transverse dynamics plot of Fig. 8, this will also result in oscillations in the $\bar{s}$ frame. Note also that both oscillations in Fig. 8 have the same period.

V. SUMMARY AND DISCUSSION

In this paper, analytical and numerical studies of bending of laser light in a curved plasma channel have been presented. In Sec. III, laser pulse envelope dynamics in a plasma channel has been studied in the paraxial approximation. Pulse propagation in a channel with a relatively small radius of curvature and a realistic plasma density profile has been simulated to demonstrate how large-amplitude centroid oscillations can lead to attenuation. Off-axis injection of the laser pulse around its equilibrium position has been proposed as a means of avoiding these centroid oscillations, as illustrated in Fig. 4. In Sec. III, relativistic self-focusing and its effect on the equilibrium position and spot size have also been discussed. The equilibrium position has been found to shift outward and the equilibrium spot size to decrease with increasing pulse intensity. In Sec. IV finite pulse length effects and wakefields have been included. A near-resonant pulse length has been chosen and it has been found that the longitudinal envelope dynamics are very similar to those of a pulse in a straight channel. The simulation results for the transverse envelope dynamics have been found to be similar to the results in the paraxial approximation, except for a drift of the laser pulse centroid towards the channel axis, which we have explained as a wakefield effect.

We now discuss the possible use of a curved plasma channel for multistage laser wakefield acceleration. First of all, it is instructive to compare the channel circumference $2\pi R$ to the length of a single acceleration stage. This length is given by the *dephasing length* $2\pi c\omega_0^2/\omega_{p0}^3$,[21] which is the distance that the laser pulse travels during the slippage of electrons from the accelerating part of the wakefield into the decelerating part, which results from the difference between the electron and laser pulse velocities. From the condition that the laser pulse remains confined in the channel, one deduces the number of dephasing lengths in a circumference to be much larger than $\omega_{p0}r_c/c$, which itself is usually larger than 1. This implies that, unless one finds a way around the dephasing problem,[22,23] one can give only a slight bend to the laser light in a single acceleration stage. From the confinement condition one also finds the number of centroid oscillations that the laser pulse undergoes during one roundtrip, which is found to be larger than ω_0/ω_{p0}; i.e., much larger than 1. The ratio of the above expressions, which can be larger or smaller than 1 depending on the parameters, determines the number of centroid oscillations that the laser pulse undergoes in one acceleration stage. At constant r_c, this number scales inversely proportional to plasma density. If it is much larger than 1, it may be advisable to use the injection strategy proposed in Sec. III to avoid centroid oscillations altogether. It is also important that we consider the *pump depletion length*, i.e., the distance at which the coupling of the laser pulse to the plasma wave starts to lead to strong pulse deformation, which in turn can lead to degradation of the wakefield. In our simulations (Figs. 8 and 9), this is seen to occur when a pronounced peak is formed at around $ct=13$ cm. In the linear regime ($a_0 \ll 1$), the pump depletion length is much longer than the dephasing length, by a factor proportional to $1/a_0^2$.[21] This implies that, during a single acceleration stage, the laser pulse shape does not change much and the wakefield does not degrade. The downside is low efficiency, as only a fraction of the laser pulse energy gets transferred to the plasma. Interestingly, the same $1/a_0^2$-scaling holds in the weakly and strongly nonlinear regimes,[19] so in this case the pump depletion length can be equal to the dephasing length or even shorter,[24] and the acceleration becomes more energy efficient. However, as pointed out before, bending laser pulses in plasma channels becomes problematic for intense laser pulses due to strong self-focusing. Finally, it should be mentioned that not only

the laser pulse, but also the electron bunch needs to be confined in the plasma channel during the acceleration, and the wakefield has to provide the required centrifugal force. The associated acceleration will give rise to the emission of synchrotron radiation.

ACKNOWLEDGMENT

This research is supported by EPSRC.[25]

APPENDIX: GENERALIZATION TO THREE-DIMENSIONAL GEOMETRY

If we include y dependence in the envelope equation, it becomes

$$\left\{2i\omega_0\frac{\partial}{\partial t}+2c\frac{\partial^2}{\partial s\partial t}+c^2\left(\frac{\partial^2}{\partial r^2}+\frac{1}{R+r}\frac{\partial}{\partial r}+\frac{\partial^2}{\partial y^2}\right)+\frac{R^2-(R+r)^2}{(R+r)^2}\left(c^2\frac{\partial^2}{\partial s^2}+2ic\omega_0\frac{\partial}{\partial s}-\omega_0^2\right)\right\}a=\Omega_p^2 a,$$

where $r=(x^2+z^2)^{1/2}-R$ as before. If one excludes wakefield effects for the moment, and assumes a parabolic plasma channel

$$\Omega_p^2=\omega_p^2\equiv\frac{4\pi n_0 e^2}{m_e}\left(1+\frac{r^2+y^2}{r_c^2}\right),$$

then the envelope equation shows that spot size oscillations in the r and y directions are decoupled. In this case, the injection strategy for avoiding spot size and centroid oscillations in the r direction is the same as in the two-dimensional case discussed above. If the laser pulse is sufficiently intense to excite an appreciable wakefield, then a coupling of spot size oscillations in the r and y directions becomes possible. For example, a pulse compression in the r direction will lead to an increase in intensity, which in turn causes self-focusing in the y direction. However, we specifically avoid a high pulse intensity in this paper, because the self-focusing prevents bending in plasma channels, as discussed above.

[1] P. Sprangle, E. Esarey, J. Krall, and G. Joyce, Phys. Rev. Lett. **69**, 2200 (1992).
[2] D. Spence and S. Hooker, Phys. Rev. E **63**, 015401 (2000).
[3] J. J. Rocca, V. Shlyaptsev, F. G. Tomasel, O. D. Cortázar, D. Hartshorn, and J. L. A. Chilla, Phys. Rev. Lett. **73**, 2192 (1994).
[4] A. Rundquist, C. G. Durfee III, Z. Chang, C. Herne, S. Backus, M. M. Murnane, and H. C. Kapteyn, Science **280**, 1412 (1998).
[5] Y. Ping, I. Geltner, A. Morozov, N. J. Fisch, and S. Suckewer, Phys. Rev. E **66**, 046401 (2002).
[6] W. P. Leemans, B. Nagler, A. J. Gonsalves, Cs. Tóth, K. Nakamura, C. G. R. Geddes, E. Esarey, C. B. Schroeder, and S. M. Hooker, Nat. Phys. **2**, 696 (2006).
[7] C. G. Durfee III and H. Milchberg, Phys. Rev. Lett. **71**, 2409 (1993).
[8] C. Courtois, A. Couairon, B. Cros, J. R. Marquès, and G. Matthieussent, Phys. Plasmas **8**, 3445 (2001).
[9] G.-Z. Sun, E. Ott, Y. C. Lee, and P. Guzdar, Phys. Fluids **30**, 526 (1987).
[10] E. Esarey, P. Sprangle, J. Krall, A. Ting, and G. Joyce, Phys. Fluids B **5**, 2690 (1993).
[11] Y. Ehrlich, C. Cohen, A. Zigler, J. Krall, P. Sprangle, and E. Esarey, Phys. Rev. Lett. **77**, 4186 (1996).
[12] J. H. Cooley, T. M. Antonsen, Jr., C. Huang, V. Decyk, S. Wang, E. Dodd, C. Ren, W. B. Mori, and T. Katsouleas, AIP Conf. Proc. **647**, 232 (2002).
[13] N. A. Bobrova, A. A. Esaulov, J.-I. Sakai, P. V. Sasorov, D. J. Spence, A. Butler, S. M. Hooker, and S. V. Bulanov, Phys. Rev. E **65**, 016407 (2002).
[14] B. H. P. Broks, K. Garloff, and J. J. A. M. van der Mullen, Phys. Rev. E **71**, 016401 (2005).
[15] T. Kurki-Suonio, P. J. Morrison, and T. Tajima, Phys. Rev. A **40**, 3230 (1989).
[16] B. Hafizi, A. Ting, P. Sprangle, and R. F. Hubbard, Phys. Rev. E **62**, 4120 (2000).
[17] N. E. Andreev, L. M. Gorbunov, V. I. Kirsanov, K. Nakajima, and A. Ogata, Phys. Plasmas **4**, 1145 (1997).
[18] P. Sprangle, J. Krall, and E. Esarey, Phys. Rev. Lett. **73**, 3544 (1994).
[19] D. F. Gordon, B. Hafizi, R. F. Hubbard, J. R. Peñano, P. Sprangle, and A. Ting, Phys. Rev. Lett. **90**, 215001 (2003).
[20] S. V. Bulanov, I. N. Inovenkov, V. I. Kirsanov, N. M. Naumova, and A. S. Sakharov, Phys. Fluids B **4**, 1935 (1992).
[21] R. F. Hubbard, P. Sprangle, and B. Hafizi, IEEE Trans. Plasma Sci. **28**, 1159 (2000).
[22] P. Sprangle, B. Hafizi, J. R. Peñano, R. F. Hubbard, A. Ting, C. I. Moore, D. F. Gordon, A. Zigler, D. Kaganovich, and T. M. Antonsen, Jr., Phys. Rev. E **63**, 056405 (2001).
[23] G. Fubiani, E. Esarey, C. B. Schroeder, and W. P. Leemans, Phys. Rev. E **73**, 026402 (2006).
[24] A. J. W. Reitsma, R. A. Cairns, R. Bingham, and D. A. Jaroszynski, Phys. Rev. Lett. **94**, 085004 (2005).
[25] http://www.epsrc.ac.uk/default.html